

Polymorphism in α -sexithiophene crystals: Relative stability and transition path

Bernhard Klett,^{1,2} Caterina Cocchi,^{1,2} Linus Pithan,¹ Stefan Kowarik,¹ and Claudia Draxl^{1,2}

¹*Institut für Physik, Humboldt-Universität zu Berlin, Berlin, Germany*

²*IRIS Adlershof, Humboldt-Universität zu Berlin, Berlin, Germany*

(Dated: February 15, 2016)

We present a joint theoretical and experimental study to investigate polymorphism in α -sexithiophene (6T) crystals. By means of density-functional theory calculations, we clarify that the low-temperature phase is favorable over the high-temperature one, with higher relative stability by about 50 meV/molecule. This result is in agreement with our thermal desorption measurements. We also propose a transition path between the high- and low-temperature 6T polymorphs, estimating an upper bound for the energy barrier of about 1 eV/molecule. The analysis of the electronic properties of the investigated 6T crystal structures complements our study.

PACS numbers: 71.15.Mb, 71.15.Nc, 71.20.Rv

I. INTRODUCTION

Organic crystalline semiconductors are promising materials for a variety of devices, ranging from light emitting diodes [1, 2] to photovoltaics [3], and field-effect transistors [4]. The possibility of synthesizing and processing these systems at low temperature and in solution is a particularly attractive feature [5]. For these reasons, organic crystals have attracted considerable interest in the last few decades. Depending on size and chemical composition of the molecular components as well as on the packing arrangement, it is possible to design systems with optimized properties.

Oligothiophenes represent a well-known family of organic crystals, which has been largely studied in view of opto-electronic applications [6, 7]. While the shortest thiophene oligomers are not suitable for device applications, due to their large band gap, most interest is devoted to longer chains such as α -sexithiophene (6T). This material presents, in fact, a favorable combination of relatively high charge-carrier mobility [8–11] and visible light absorption [12–17], which makes it a very promising compound for organic electronics.

The weak interactions between 6T molecules enable the growth of two crystal structures, which are referred to as high- and low-temperature (HT and LT) phases [18, 19]. Both exhibit herringbone packing, with either two (HT) or four (LT) molecules per unit cell. Polymorphism, i.e., the presence of two or more possible arrangements of the molecules in the solid state [20], is often observed in organic crystals. The coexistence of different morphologies of molecules in their crystal phases may strongly influence the properties of such materials [21–23]. This has practical impact not only in condensed-matter physics and materials science [24, 25], but also in biochemistry and pharmacology [26, 27], where polymorphism is known to crucially affect drug formulation and stability. Hence, a clear understanding of the fundamental mechanisms ruling this phenomenon is desired in view of tailoring molecular materials with customized features.

In this paper, we address the question of polymorphism in 6T with a joint theoretical and experimental study. Specifically, we aim to determine which of the experimentally observed phases is the more stable one. To do so, we combine a first-principle approach, based on density-functional theory (DFT) and including van der Waals interactions, with thermal desorption measurements. Moreover, we propose and analyze a possible transition path from one structure to the other, and estimate the size of the corresponding energy barrier. The information about the crystal structure is complemented by an analysis of the electronic properties of selected systems along the transition path.

The paper is organized as follows: In Sec. II, we introduce the HT and LT polymorphs of 6T and the theoretical and experimental methods that we use. Sec. III addresses the relative stability of the two known polymorphs, both theoretically and experimentally. In Sec. IV, we discuss the transition path and the electronic properties corresponding to several structures along that path.

II. SYSTEMS AND METHODS

A. Sexithiophene crystals

The building blocks of 6T crystals are planar molecules, consisting of carbon, hydrogen, and sulfur atoms, which are arranged in a chain of six rings. Sexithiophene exhibits a herringbone arrangement of the molecules in its crystal phases [18, 19]. The monoclinic unit cells of the LT and HT polymorphs are shown in Fig. 1. The corresponding structural parameters, based on x-ray diffraction experiments [18, 19], are listed in Tab. I. In the LT phase (left), the unit cell belongs to the space group $P2_1/n$, with a monoclinic angle $\beta_{LT} = 90.8^\circ$ and contains four molecules, arranged in such a way, that the long molecular axes are almost parallel to each other. In this configuration, the tilt angle $\phi_{LT} = 66.5^\circ$ is defined between the long molecular axis and the ab plane,

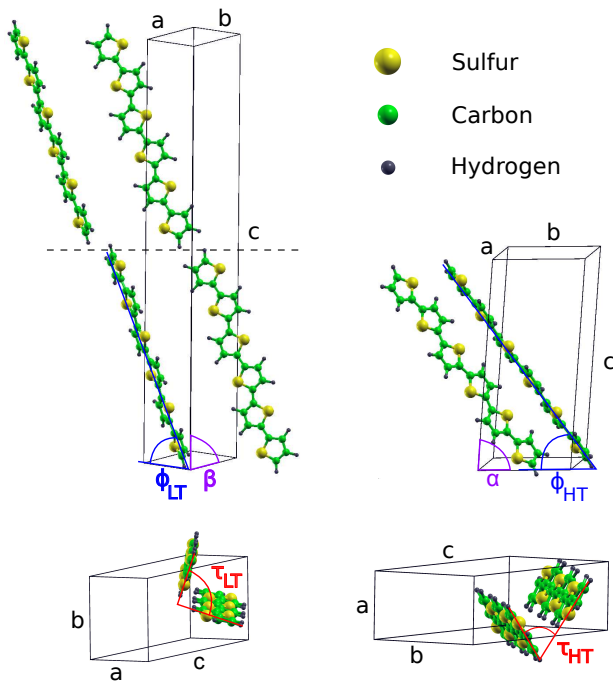


FIG. 1: (color online) Unit cells of LT (left) and HT (right) polymorphs of 6T. Lattice parameters a , b , c , as well as tilt (ϕ), herringbone (τ), and monoclinic angles (α/β) are indicated. The dashed line marks the plane, which divides the unit cell of the LT polymorph in half.

	a [Å]	b [Å]	c [Å]	α/β [deg]	ϕ [deg]	τ [deg]
HT	5.68	9.14	20.67	97.8	48.5	55.0
I	5.75	8.88	21.01		52.1	57.2
II	5.79	8.75	21.17		53.9	58.3
III	5.82	8.62	21.34		55.7	59.4
IV	5.89	8.37	21.68		59.3	61.6
V	5.93	8.24	21.85		61.1	62.7
VI	5.96	8.11	22.01		62.9	63.8
LT	6.03	7.85	22.35	90.8	66.5	66.0

TABLE I: Structural parameters of the HT and LT polymorphs as well as of intermeditate structures (see Sec. IV A). The lattice parameters of the LT polymorph are referred to the reduced unit cell (see Sec. III). Lattice constants a , b and c , as well as the monoclinic angles α/β , the tilt angle ϕ , and the herringbone angle τ are displayed.

with lattice parameters $a = 6.03$ Å and $b = 7.85$ Å. The herringbone angle τ_{LT} between the short molecular axes adopts a value of 66° (bottom-left of Fig. 1).

The HT structure is shown on the right-hand side of Fig. 1. Also in this case a and b have comparable values ($a = 5.68$ Å, $b = 9.14$ Å), while c is much larger, being 20.67 Å. Note that we have permuted the crystal axes to highlight the similarity with the LT phase and to facilitate the construction of the transition path between them (see Sec. IV) [28]. The space group for this structure is $P2_1/b$, with $\alpha_{HT} = 97.8^\circ$. The volume of the HT unit cell is half as large as the LT one and accommodates two

inequivalent molecules. Again, the long molecular axes are approximately parallel to each other. Both, the herringbone and tilt angle, that is defined with respect to the ab plane, have smaller values than in the LT phase, being 55° and 48.5° , respectively (see also Tab. I).

B. Computational details

Total-energy and force calculations are performed within the framework of DFT. All calculations are carried out with the full-potential all-electron code `exciting` [29], implementing the (linearized) augmented plane-wave plus local orbitals method.

A plane-wave cutoff $G_{max} \approx 4.7$ bohr $^{-1}$ is adopted for minimizing the atomic forces. This value corresponds to $R_{min}^{MT} G_{max} = 3.5$, where $R_{min}^{MT} = 0.75$ bohr is the smallest muffin-tin radius, corresponding to hydrogen. Radii of 1.15 bohr and 1.80 bohr are used for carbon and sulfur, respectively. To evaluate the small energy difference between the two polymorphs, we further increase the plane-wave cutoff to $G_{max} \approx 6.7$ bohr $^{-1}$, corresponding to $R_{min}^{MT} G_{max} = 5.0$. We use $1 \times 5 \times 3$ and $4 \times 3 \times 1$ \mathbf{k} -point grids for HT and LT, respectively. These parameters ensure the convergence of total energies within 0.4 meV/molecule.

For most calculations, we adopt the local density approximation (LDA), using the Perdew-Wang exchange-correlation functional [30]. The internal geometry is optimized by minimizing the atomic forces until they are smaller than 25 meV/Å. The lattice parameters are thereby fixed at their experimental values (see Tab. I). Doing so, the internal geometry depends largely on the electrostatic interactions. These are well described by LDA, as confirmed by the agreement of the interatomic distances with those reported in Ref. [31]. Similar results have been found in an earlier study of anthracene [32].

To check the reliability of the LDA results and obtain more accurate energy differences between the two polymorphs, we also employ the DFT-D2 method [33] on top of the Perdew-Burke-Ernzerhof (PBE) exchange-correlation functional [34] to calculate the total energies of the HT and LT polymorphs.

C. Experimental methods

We grow 6T films by thermal evaporation in an organic molecular beam deposition vacuum chamber equipped with a beryllium window for *in situ* x-ray measurements at a base pressure of $7 \cdot 10^{-7}$ mbar. Cleaved KCl substrates are heated up to 420°C in vacuum to reduce surface contamination prior to the deposition. The films are grown with molecular deposition rates between 1 and 1.5 Å/min at 50°C substrate temperature to a thickness of 150 ± 20 Å. The film thickness is monitored with a quartz crystal microbalance during growth. The grown thin films are analyzed by means of x-ray diffraction in a

$\theta - 2\theta$ geometry, in which the reflectivity in dependence of the out-of-plane scattering vector $q_z = \frac{4\pi}{\lambda} \sin \theta$ is studied at the corresponding values of the different crystal phases. The measurements are performed at a $Cu K_\alpha$ rotating anode system with a wavelength of $\lambda = 1.5406 \text{ \AA}$ in nitrogen atmosphere. Using a temperature controlled stage we heat the substrate to evaluate molecular desorption from the decreasing intensity of the Bragg reflections of the LT and HT crystal phases. After reaching the desired temperature, we first monitor the x-ray reflection intensity of the HT phase at $q_z = 0.907 \text{ \AA}^{-1}$ and subsequently the reflection of the LT phase at $q_z = 0.838 \text{ \AA}^{-1}$.

III. RELATIVE STABILITY OF HT AND LT POLYMORPHS

The large LT unit cell is almost symmetrical with respect to a plane parallel to the ab plane, as indicated in Fig. 1. Thus the unit cell can be approximately divided into two halves, with lattice constants a , b , and $c = 22.35 \text{ \AA}$, containing two molecules each. The total energies of these smaller structures, obtained after minimizing the atomic forces, differ by less than 0.2 meV/molecule. Since this value is within our computational accuracy (see Sec. II B), we can consider the LT polymorph in such reduced unit cell [35]. This allows us to significantly decrease the computational costs, ensuring the same numerical accuracy for both polymorphs. In the remainder of this article the label LT will refer to the reduced unit cell.

The relative stability of the HT and LT polymorphs is determined by their total energies. By employing the LDA functional, we find the LT phase to be more stable by 36 meV/molecule, compared to the HT phase. This energy difference increases to 51 meV/molecule, when we explicitly account for van der Waals interaction using the DFT-D2 method. This shows that both functionals lead to the same qualitative picture.

Experimentally, we determine the more stable phase, as well as the difference in the desorption energy barrier E_d of the two crystal structures, by measuring the desorption rates of both LT and HT phase crystallites at fixed temperatures. A 15 nm thick, polycrystalline 6T thin film on NaCl exhibits phase coexistence as seen from the characteristic $(006)_{LT}$ and $(003)_{HT}$ Bragg reflections that both occur in a $\Theta - 2\Theta$ scan (see Figure 2, inset). Heating this 6T film to a temperature of $428 \pm 5 \text{ K}$, corresponding to the onset of molecular desorption, we observe that the intensities of the Bragg reflections drop linearly as shown in Figure 2. Interestingly, the HT phase desorbs at a faster rate [$R^{HT} = (1.531 \pm 0.050) \cdot 10^{-4} \text{ s}^{-1}$] than the LT phase [$R^{LT} = (1.000 \pm 0.011) \cdot 10^{-4} \text{ s}^{-1}$], indicating a higher stability of the LT phase.

For a quantitative analysis, we explain the differences between the temporal decay of the two Bragg intensities by a difference in desorption energy barriers E_d . Assum-

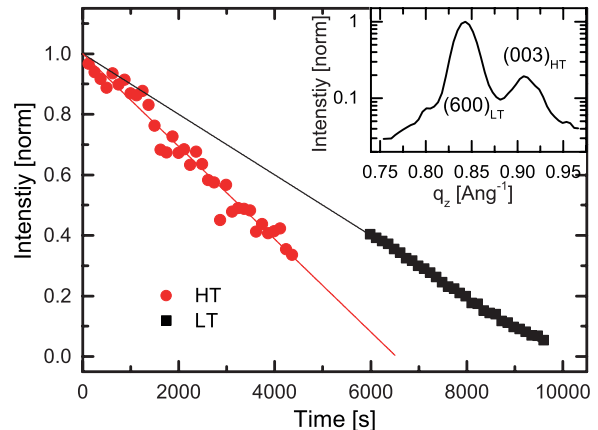


FIG. 2: (color online) Decay of the HT and LT Bragg reflection intensities over time at a substrate temperature $T = 428 \pm 5 \text{ K}$. Inset: $\Theta - 2\Theta$ scan of the monitored LT and HT reflections.

ing that the Bragg intensity is directly proportional to the respective amount of HT or LT phase, the constant slope of the decay curves can be explained by molecular desorption from step edges at a constant rate without any significant morphological changes of HT and LT islands. In atomic force microscopy measurements, resolving molecular terraces of standing upright molecules, we find no distinctly different HT and LT islands, so that a similar geometry is assumed for both phases. We use an Arrhenius-type relation of the desorption rate $R = -A e^{-E_d/k_B T}$ with the molecular desorption energy E_d , the (constant) temperature T , and an attempt frequency A . Assuming $A = A^{LT} = A^{HT}$ for both phases, one can write

$$\ln \left(\frac{R^{HT}}{R^{LT}} \right) = -\frac{E_d^{HT}}{k_B T} + \frac{E_d^{LT}}{k_B T}. \quad (1)$$

Therefore the desorption energy difference $\Delta E_d = E_d^{LT} - E_d^{HT}$ is given by

$$\Delta E = \ln \left(\frac{R^{HT}}{R^{LT}} \right) \cdot k_B T. \quad (2)$$

From the decay rates we estimate $\Delta E_d = 15.7 \pm 3.1 \text{ meV}$ between the two phases. This finding is in qualitative agreement with theory, however, the energy difference is about 3 times smaller than the computed difference in relative stability. We can identify two possible sources of such discrepancy. Most important, the process of thermal desorption occurs at the surface and in particular at step edges and corners. In this case each molecule interacts only with a reduced number of nearest neighbors compared to the bulk, and therefore the resulting binding energy is intrinsically lower. Moreover, DFT calculations do not take into account thermodynamical effects. Although most of these contributions cancel out when considering energy differences, they still may lead to a

systematic overestimation of the experimental values, as previously pointed out for other organic crystals [36]. Overall, we claim good agreement between our theoretical and experimental results, which identify the LT phase as the more stable one. It is finally worth mentioning that our result is in contrast with a previous work based on classical force-fields calculations [37]. In that case, the authors found the HT polymorph to be energetically favored with respect to LT by about 15 meV/molecule. Although the absolute value of this difference is rather small, we can attribute the better accuracy and, importantly, the correct sign of our result to the inclusion of quantum effects.

IV. TRANSITION PATH BETWEEN HT AND LT PHASES

A. Construction of the path

In Sec. III we have clarified the higher relative stability of the LT polymorph with respect to the HT one. However, the energy difference between the two polymorphs is not the only factor that determines the material to grow in one phase rather than the other. One aspect is that film growth not only involves thermodynamical stability, but also kinetic processes. A quantity of interest in this context is the energy required to transform one structure into the other. To this extent we propose a possible transition path. Thereby, we face the challenge of determining the intermediate structures. While a variety of methods have been proposed and employed for such purpose [38], only a few of them can be applied to molecular crystals. In fact, in these systems molecules should keep their shape and be able to reorient themselves with respect to each other, while the unit cell adjusts accordingly. To fulfill these requirements, we adopt the so-called *drag* method [39]. In our case, we treat molecules as rigid, while interpolating lattice parameters, as well as herringbone and tilt angles, the latter defining the orientation of the molecules with respect to each other and to the unit cell, respectively.

Six intermediate structures are constructed and shown in Fig. 3a, labeled from I to VI. In Tab. I, lattice constants, as well as herringbone and tilt angles are reported. For comparison, also the structural parameters of the HT and LT phase are shown, highlighted in bold. It is worth noting that interpolation of a , b , c , ϕ and τ , indirectly determines the angles between the lattice parameters. Hence, while the initial HT and LT structures are monoclinic, the intermediate ones become triclinic. By inspecting Fig. 3a the variation of herringbone and tilt angles is visible, as well as the change of the lattice parameters. The six intermediate structures are optimized to minimize the atomic forces, while the unit cell parameters are held fixed to the values reported in Tab. I.

B. Relative stabilities and electronic structure

	HT	I	II	III	IV	V	VI	LT
LDA	36.2	42.2	582.3	687.4	601.1	517.4	16.8	0.0
vdW	51.0							0.0

TABLE II: Energy difference per molecule of each structure with respect to the LT phase, as obtained from LDA and DFT-D2 (labeled vdW). All energies are given in meV/molecule.

As a next step, we evaluate the total energies of the optimized intermediate structures. In this way, we are able to estimate the energy barrier between the HT and LT phases. The results of these calculations are reported in Tab. II and in Fig. 3b. The relative energies with respect to the most stable polymorph, the LT phase, are displayed as a function of the reaction coordinate Ω , which is defined by the lattice parameters and the angles τ and ϕ . Overall the barrier presents a *top hat* shape. While structure I resembles the HT phase and is energetically very close to it, structure VI is similar in energy and shape to the LT phase (see Tab. II). On the other hand, structures II-V are significantly less favored, exhibiting energies more than 0.5 eV/molecule higher compared to LT. The most unfavored polymorph is structure III. The total energy exceeds that of the LT phase by about 0.7 eV per molecule, which represents the apex of the dome. Considering an increase in energy by explicitly accounting for van der Waals interactions, we estimate the upper bound of the barrier to be about 1 eV. Similar results have been obtained for other organic crystals, such as *para*-sexiphenyl on a mica step-edge [40].

We finally present, in Fig. 4, the electronic properties of selected intermediate structures, compared to the HT and LT ones. These results allow us to further characterize the predicted metastable structures. In Fig. 4 the band structure and density of states (DOS) of the three selected intermediates I, IV and VI are shown in comparison with the stable polymorphs HT and LT. We notice the typical features of organic crystals (see e.g. Ref. [41]). In both the valence and conduction regions, subbands are arranged in pairs, according to the double multiplicity of the 6T molecules in the unit cell. These features are reflected also in the DOS, which presents in both cases relatively sharp peaks in the valence region, corresponding to the different subbands. The subbands in the conduction region are energetically closer to each other, and present overall increased dispersion compared to the valence region. The highest valence-bands (VB) and lowest conduction-bands (CB) are highlighted in green. Both polymorphs have indirect Kohn-Sham (KS) band gaps of 1.2 and 1.1 eV for LT and HT, respectively.

In the LT phase the VB bandwidth is 0.2 eV, while it is larger (0.5 eV) in the CB. For symmetry reasons, both bands are degenerate along the path from Y to C , and

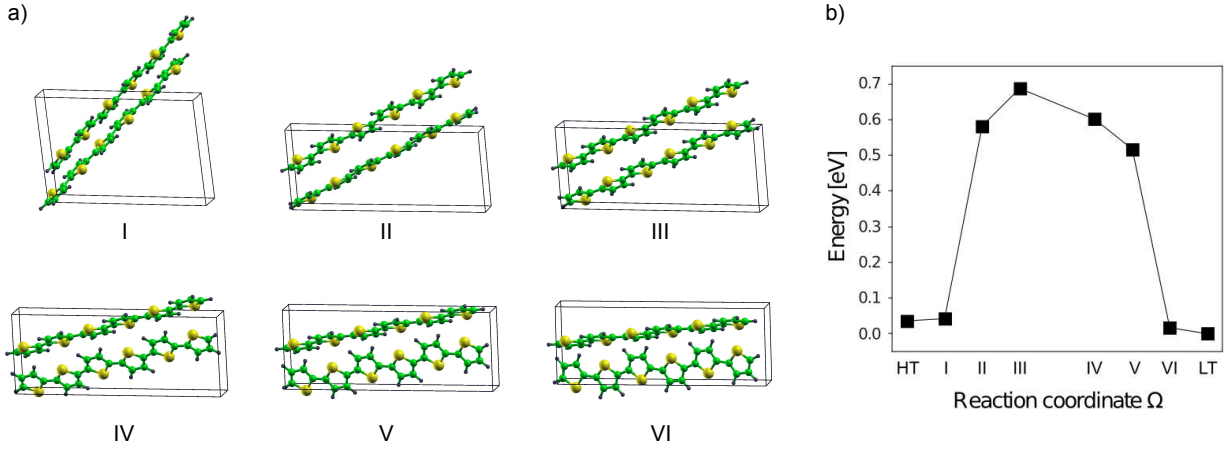


FIG. 3: (color online) a) Intermediate structures along the proposed transition path (see also Tab. I). b) Energy barrier between HT and LT polymorphs of 6T. The reaction coordinate Ω is a function of the lattice parameters a , b , and c , as well as the angles ϕ and τ .

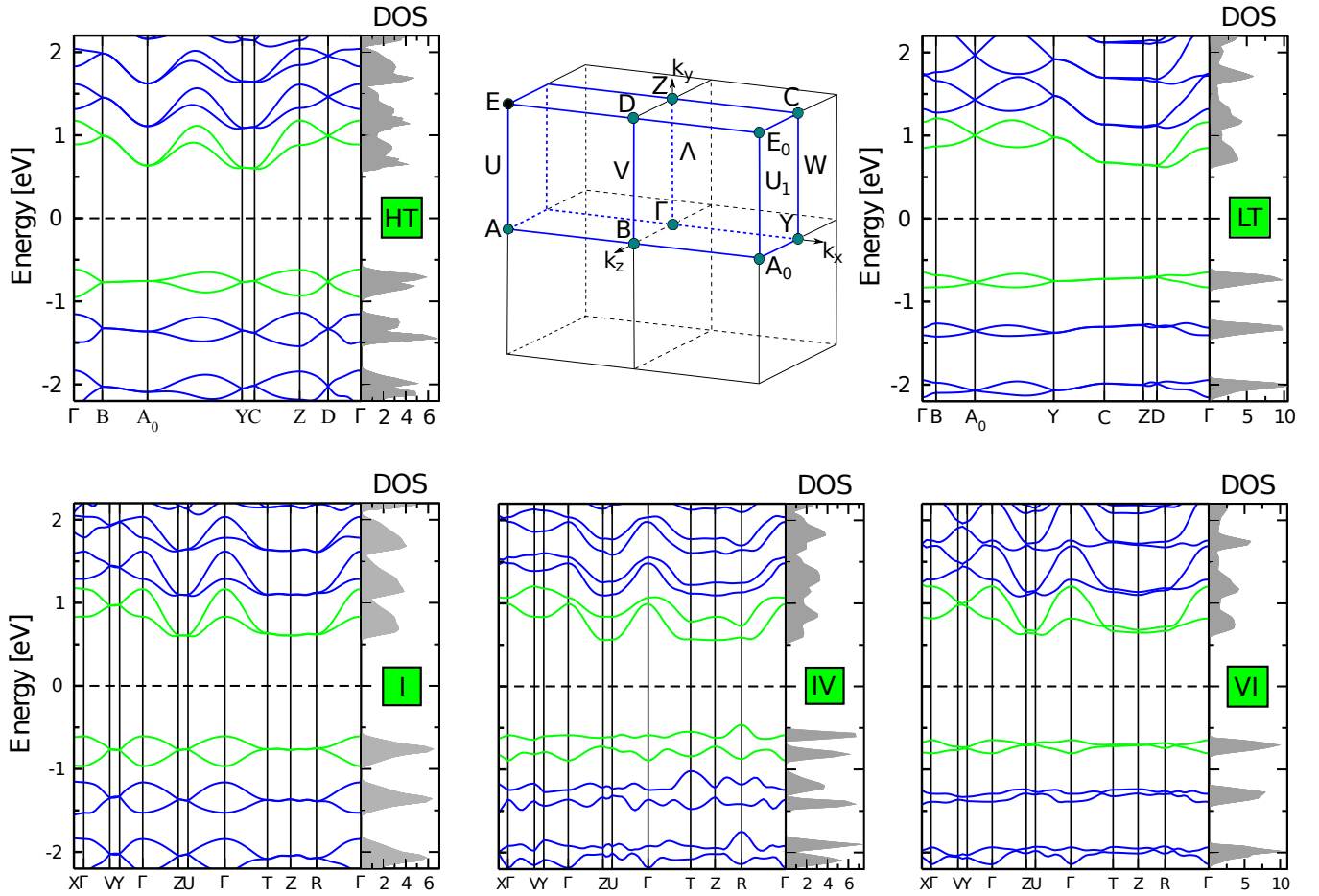


FIG. 4: (color online) Band structure and density of states (DOS) of HT and LT, as well as selected intermediate structures (see Fig. 3). The subbands corresponding to the uppermost valence-band (VB) pair and lowest conduction-band (CB) pair are highlighted in green. The Brillouin zone of HT and LT is shown in the middle of the top row. The DOS are expressed in 100 states/eV. The Fermi energy is set to 0 eV.

exhibit a small splitting between C and Z . The splitting is largest at the Γ -point and halfway inbetween the points A_0 and Y . In the HT phase, the bandwidth is twice as large in the VB (0.4 eV), and slightly larger in the CB (0.6 eV), compared to LT. The largest splitting is found at Γ and Z , as well as halfway between A_0 and Y . Bands are degenerate between Y and C , as well as between B and A_0 .

For comparison, we have selected those structures (I, IV and VI), which mostly differ from each other in the arrangement of the molecules and in the energetics (see Figs. 3a and b). These intermediate structures belong to the space group $P1$, exhibiting trivial symmetry. These systems present indirect KS band gaps of 1.0 eV (I), 0.9 eV (IV), and 1.2 eV (VI). These values are comparable to those of the HT (1.1 eV) and LT (1.2 eV) phases. The lower stabilities of these systems with respect to the stable HT and LT polymorphs is evident from the band structures. In particular, in structure IV, which is clearly unfavored in the chosen transition path, a large band splitting is observed, in both valence and conduction regions. Especially the occupied states feature sharp peaks in the DOS. This is a signature of the lower symmetry of this system, compared to the stable HT and LT polymorphs. The other intermediate structures, I and VI, which are structurally and energetically close to HT and LT, respectively, still present subbands, and the fingerprints of reduced symmetry, such as subband degeneracy, are less pronounced. Overall, the bands exhibit low dispersion, especially for the IV and VI structures. This implies high effective carrier masses and therefore low charge-carrier mobilities in these regions. The bandwidths in the VBs decrease from 0.4 eV for I and IV to 0.2 eV in structure VI. Thus, structure I (VI) shares the same bandwidth in the VB as the HT (LT) polymorph. The CB bandwidths tend to be larger with values of 0.6 eV (structure I), 0.7 eV (structure IV) and 0.7 eV (structure VI), thus they are 0.1 eV larger than those of the HT and LT phase, respectively.

V. SUMMARY AND CONCLUSIONS

We have presented a combined theoretical and experimental study on polymorphism in 6T crystals. We have clarified that the LT phase is favored over the HT one by about 50 meV/molecule, as obtained from DFT calculations, explicitly taking into account van der Waals interactions. This result is in agreement with our thermal desorption measurements. Our results confirm the importance of explicitly accounting for quantum effects and dispersive intermolecular interactions, to quantify the relative stability of different polymorphs in organic crystal structures.

In addition, we have proposed a transition path between the two stable 6T polymorphs, estimating the energy barrier between the HT and LT phase of about 1 eV/molecule. The results are supplemented by a thorough analysis of the electronic properties of the stable and selected intermediate structures.

Acknowledgement

We acknowledge fruitful discussions with Hong Li, Dmitrii Nabok, and Peter Schäfer. This work was partly funded by the German Research Foundation (DFG) through the Collaborative Research Centers SFB 658 and SFB 951. C. C. acknowledges support from the Berliner Chancengleichheitsprogramm (BCP). L. P. acknowledges support from the Studienstiftung des deutschen Volkes.

-
- [1] S. R. Forrest, *The road to high efficiency organic light emitting devices*, Org. Electron. **4** (2003) (23), pp. 45–48
 - [2] S. R. Forrest, *The path to ubiquitous and low-cost organic electronic appliances on plastic*, Nature **428** (2004) (6986), pp. 911–918
 - [3] P. Peumans, A. Yakimov and S. R. Forrest, *Small molecular weight organic thin-film photodetectors and solar cells*, J. Appl. Phys. **93** (2003) (7), pp. 3693–3723
 - [4] M. Muccini, *A bright future for organic field-effect transistors*, Nature Mat. **5** (2006) (8), pp. 605–613
 - [5] J. Fraxedas, *Molecular Organic Materials: From Molecules to Crystalline Solids* (Cambridge University Press, 2006)
 - [6] O. Dippel, V. Brandl, H. Bässler, R. Danieli, R. Zamboni and C. Taliani, *Energy-dependent branching between fluorescence and singlet exciton dissociation in sexithienyl thin films*, Chem. Phys. Lett. **216** (1993) (3), pp. 418–423
 - [7] R. Marks, F. Biscarini, R. Zamboni and C. Taliani, *Polarised electroluminescence from vacuum-grown organic light-emitting diodes*, Europhys. Lett. **32** (1995) (6), pp. 523–528
 - [8] G. Horowitz, D. Fichou and F. Garnier, *Alpha-sexithienyl: a p-and n-type dopable molecular semiconductor*, Solid State Commun. **70** (1989) (3), pp. 385–388
 - [9] H. Akimichi, K. Waragai, S. Hotta, H. Kano and H. Sakaki, *Field-effect transistors using alkyl substituted oligothiophenes*, Appl. Phys. Lett. **58** (1991) (14), pp. 1500–1502
 - [10] H. Katz, L. Torsi and A. Dodabalapur, *Synthesis, material properties, and transistor performance of highly pure thiophene oligomers*, Chem. Mater. **7** (1995) (12), pp. 2235–2237
 - [11] G. Horowitz, R. Hajlaoui and F. Kouki, *An analytical model for the organic field-effect transistor in the depletion mode. Application to sexithiophene films and single crystals*, Eur. Phys. J. - Appl. Phys. **1** (1998) (03), pp.

- 361–367
- [12] D. Oeter, H.-J. Egelhaaf, C. Ziegler, D. Oelkrug and W. Göpel, *Electronic transitions in α -oligothiophene thin films. Comparison of ultraviolet/visible absorption spectroscopy and high resolution electron energy loss spectroscopy investigations*, J. Chem. Phys. **101** (1994) (7), pp. 6344–6352
- [13] D. Oelkrug, H.-J. Egelhaaf and J. Haiber, *Electronic spectra of self-organized oligothiophene films with standing and lying molecular units*, Thin Solid Films **284** (1996), pp. 267–270
- [14] Y. Kanemitsu, N. Shimizu, K. Suzuki, Y. Shiraishi and M. Kuroda, *Optical and structural properties of oligothiophene crystalline films*, Phys. Rev. B **54** (1996) (3), pp. 2198–2204
- [15] D. Fichou, *Structural order in conjugated oligothiophenes and its implications on opto-electronic devices*, J. Mater. Chem. **10** (2000) (3), pp. 571–588
- [16] R. Marks, R. Michel, W. Gebauer, R. Zamboni, C. Taliani, R. Mahrt and M. Hopmeier, *The origin of photoluminescence from α -sexithienyl thin films*, J. Phys. Chem. B **102** (1998) (39), pp. 7563–7567
- [17] L. Pithan, C. Cocchi, H. Zschiesche, C. Weber, A. Zykov, S. Bommel, S. J. Leake, P. Schäfer, C. Draxl and S. Kowarik, *Light Controls Polymorphism in Thin Films of Sexithiophene*, Cryst. Growth Des. **15** (2015), pp. 1319–1324
- [18] T. Siegrist, R. Fleming, R. Haddon, R. Laudise, A. Lovinger, H. Katz, P. Bridenbaugh and D. Davis, *The crystal structure of the high-temperature polymorph of α -hexathienyl (α -6T/HT)*, J. Mater. Res. **10** (1995) (09), pp. 2170–2173
- [19] G. Horowitz, B. Bacht, A. Yassar, P. Lang, F. Demanze, J.-L. Fave and F. Garnier, *Growth and Characterization of Sexithiophene Single Crystals*, Chem. Mater. **7** (1995) (7), pp. 1337–1341
- [20] G. R. Desiraju, *Polymorphism: the same and not quite the same*, Cryst. Growth Des. **8** (2008) (1), pp. 3–5
- [21] J. Bernstein, *Crystal growth, polymorphism and structure-property relationships in organic crystals*, J. Phys. D **26** (1993), pp. B66–B76
- [22] M. R. Cairn, *Crystalline polymorphism of organic compounds*, Top. Curr. Chem. **198** (1998), pp. 163–208
- [23] C. Lorch, R. Banerjee, C. Frank, J. Dieterle, A. Hinderhofer, A. Gerlach and F. Schreiber, *Growth of Competing Crystal Phases of -Sexithiophene Studied by Real-Time in Situ X-ray Scattering*, J. Phys. Chem. C **119** (2015) (1), pp. 819–825
- [24] T. L. Threlfall, *Analysis of organic polymorphs. A review*, Analyst **120** (1995) (10), pp. 2435–2460
- [25] D. Braga, F. Grepioni and G. R. Desiraju, *Crystal engineering and organometallic architecture*, Chem. Rev. **98** (1998) (4), pp. 1375–1406
- [26] D. Giron, *Thermal analysis and calorimetric methods in the characterisation of polymorphs and solvates*, Thermochim. Acta **248** (1995), pp. 1–59
- [27] B. Rodriguez-Spong, C. P. Price, A. Jayasankar, A. J. Matzger and N. Rodriguez-Hornedo, *General principles of pharmaceutical solid polymorphism: a supramolecular perspective*, Adv. Drug Delivery Rev. **56** (2004) (3), pp. 241–274
- [28] Typically in crystallography the nomenclature for HT is such that the largest lattice parameter is labeled a and the monoclinic angle is then β . Consequently, b is the shortest lattice parameter. For the conventional nomenclature we refer to Ref. [18].
- [29] A. Gulans, S. Kontur, C. Meisenbichler, D. Nabok, P. Pavone, S. Rigamonti, S. Sagmeister, U. Werner and C. Draxl, *exciting: a full-potential all-electron package implementing density-functional theory and many-body perturbation theory*, J. Phys. Condens. Matter. **26** (2014) (36), p. 363202
- [30] J. P. Perdew and Y. Wang, *Accurate and simple analytic representation of the electron-gas correlation energy*, Phys. Rev. B **45** (1992), p. 13244
- [31] P. Hermet, J.-L. Bantignies, A. Rahmani, J.-L. Sauvajol and M. Johnson, *Polymorphism of crystalline α -quaterthiophene and α -sexithiophene: ab initio analysis and comparison with inelastic neutron scattering response*, J. Phys. Chem. A **109** (2005) (18), pp. 4202–4207
- [32] K. Hummer, P. Puschnig and C. Ambrosch-Draxl, *Ab initio study of anthracene under high pressure*, Phys. Rev. B **67** (2003) (18), p. 184105
- [33] S. Grimme, *Semiempirical GGA-type density functional constructed with a long-range dispersion correction*, J. Comput. Chem. **27** (2006), pp. 1787–1799
- [34] J. P. Perdew, K. Burke and M. Ernzerhof, *Generalized Gradient Approximation Made Simple*, Phys. Rev. Lett. **77** (1996) (18), pp. 3865–3868
- [35] We take the top half in Fig. 1. However, this choice does not affect what follows.
- [36] D. Nabok, P. Puschnig and C. Ambrosch-Draxl, *Cohesive and surface energies of p-conjugated organic molecular crystals: A first-principles study*, Phys. Rev. B **77** (2008) (24), p. 245316
- [37] R. G. Della Valle, E. Venuti, A. Brillante and A. Girlando, *Are Crystal Polymorphs Predictable? The Case of Sexithiophene*, J. Phys. Chem. A **112** (2008), p. 67156722
- [38] M. L. McKee and M. Page, *Computing Reaction Pathways on Molecular Potential Energy Surfaces*, in K. B. Lipkowitz and D. B. Boyd (eds.), *Reviews in Computational Chemistry* (John Wiley & Sons, Inc., 1993), pp. 35–65
- [39] G. Henkelman, G. Jóhannesson and H. Jónsson, *Methods for Finding Saddle Points and Minimum Energy Paths*, in S. D. Schwartz (ed.), *Theoretical Methods in Condensed Phase Chemistry* (Springer Netherlands, 2002), no. 5 in Progress in Theoretical Chemistry and Physics, pp. 269–302
- [40] G. Hlawacek, P. Puschnig, P. Frank, A. Winkler, C. Ambrosch-Draxl and C. Teichert, *Characterization of Step-Edge Barriers in Organic Thin-Film Growth*, Science **321** (2008) (5885), pp. 108–111
- [41] K. Hummer and C. Ambrosch-Draxl, *Electronic properties of oligoacenes from first principles*, Phys. Rev. B **72** (2005), p. 205205